Future Computing and Informatics Journal

Volume 2
Issue 2 (2020) *2017, Volume 2, Issue 2*

Article 5

2017

A thresholding based technique to extract retinal blood vessels from fundus images

Jyotiprava Dash
Department of Electronic & Tele-communication, Veer Surendra Sai University of Technology, Burla, 768018, India., jyotipravadash89@gmail.com

Nilamani Bhoi
Department of Electronics & Telecommunication Engineering, Veer Surendra Sai University of Technology, Burla 768018, Sambalpur, India, nilamanib@gmail.com

Available online at www.sciencedirect.com

ScienceDirect

Future Computing and Informatics Journal 2 (2017) 103–109
http://www.journals.elsevier.com/future-computing-and-informatics-journal/

A thresholding based technique to extract retinal blood vessels from fundus images

Jyotiprava Dash*, Nilamani Bhoi

Veer Surendra Sai University of Technology, Burla, Odisha, India

Received 2 June 2017; accepted 11 October 2017
Available online 28 October 2017

Abstract

Retinal imaging has become the significant tool among all the medical imaging technology, due to its capability to extract many data which is linked to various eye diseases. So, the accurate extraction of blood vessel is necessary that helps the eye care specialists and ophthalmologist to identify the diseases at the early stages. In this paper, we have proposed a computerized technique for extraction of blood vessels from fundus images. The process is conducted in three phases: (i) pre-processing where the image is enhanced using contrast limited adaptive histogram equalization and median filter, (ii) segmentation using mean-C thresholding to extract retinal blood vessels, (iii) post-processing where morphological cleaning operation is used to remove isolated pixels. The performance of the proposed method is tested on and experimental results show that our method achieve an accuracies of 0.955 and 0.954 on Digital retinal images for vessel extraction (DRIVE) and Child heart and health study in England (CHASE_DB1) databases respectively.

Keywords: Retinal imaging; Blood vessels; Mean-C; DRIVE and CHASE_DB1 databases; Medical imaging; Ophthalmologist

1. Introduction

The exponential growth of the quantity of digital images has covered the direction towards the study of computer vision [1]. Exploration in medical informatics focuses predominantly on assimilating computer technology into the practice of medicine in order to advance in the area of analysis and treatment [2]. The retinal vasculature offers facts which is used to localize the optic disc and fovea, and act as a main part for recognition of pathological changes in automated diagnostic system [3]. Fundus imaging in ophthalmology is a method for medical verdict and exploration of numerous diseases like hypertension, diabetic retinopathy, cataract, glaucoma and cardiovascular diseases [4]. In fundus image analysis the automatic extraction of object from background is an essential task. But there are certain difficulties for this such as the variability in vessel width and low resolution databases that includes nose and changes in brightness [5].

Many methods have already proposed for blood vessel segmentation by taking different databases which can be mainly categorized as: machine learning method, filtering based method and model based method. The supervised methods are coming under machine-learning methods where the pixels are marked either as vessels or non-vessels. In supervised learning, classifiers are accomplished with data from hand-labeled images [6]. In Ref. [6], the author proposed a supervised method where the image is initially enhanced and then features are extracted using 7D feature vector and to this features undergoes neural network classification for labeling the pixels as vessels or nonvessel. Finally, a post-processing step is applied for gap filling and removal of insulated pixels. Fraz et al. [7], suggested a supervised technique that utilizes a

* Corresponding author. Department of Electronic & Tele-communication, Veer Surendra Sai University of Technology, Burla, 768018, India.
E-mail addresses: jyotipravadash89@gmail.com (J. Dash), nilamanib@gmail.com (N. Bhoi).
Peer review under responsibility of the Faculty of Computers and Information, Future University in Egypt

https://doi.org/10.1016/j.fcij.2017.10.001

collaboration of bagged and boosted decision trees utilizes a feature vector to analyze both healthy and pathological images. In Ref. [8], the author introduced a method where in the earlier stage two binary images are created from green plane using high pass filtering and morphological reconstruction method. Next, the two binary image common areas are extracted as main vessels. All the remaining pixels in the two binary images are categorized using a Gaussian mixture model (GMM) with a set of eight features that are extracted based on pixel neighborhood and first and second-order gradient images. In the final post processing stage, the major vessels are joined with the classified vessel pixels. In the filtered based approach, retinal vessel segmentation is performed using morphological operators. In morphological image processing, the form is known priory which generates a structuring element that is used for filtering the objects from the background [5]. In Ref. [5] the author developed a new method for identification of blood vessels. This method segments the large blood vessels as a solid structure without artifacts. A methodology that includes vessel skeletal recognition with morphological bit planes for segmentation of retinal blood vessels is offered by Fraz et al. [9]. An automated novel segmentation method has been introduced by Azzopardi et al. [10]. It is based on the combination of receptive fields (CORF) raking model of a simple cell in the visual cortex and its employment called combination of shifted filter responses (COSFIRE). For the extraction of retinal blood vessels a rod-shaped COSFIRE non-linear filter is used. In Ref. [11], the author introduced a system that utilizes the conception of matched filter with first order derivative of Gaussian considering that the vessel cross section is a symmetric Gaussian function. To extract the blood vessels a pair of zero mean Gaussian filter and the first order derivative of Gaussian is used. Roychowdhury et al. [12], presents a first-hand method where the new pixels generated iteratively by adaptive global thresholding for vessel approximations. A stopping condition is used to dismiss the iterative vessel addition process and hence reduce the false positives. In model based approach, a vessel model is useful to identify the retinal blood vessels. These approaches are sensitive to their parameterization. Here, the trouble is that the parameters should be selected sensibly to extract thin and large vessels at once [13]. In Ref. [14], a structure is used where initially the Hessian method is used to segment the blood vessels from the rescaled image and after this again it is back sampled to original size. Subsequently blood vessels are take-out using Hysteresis thresholding. At the last stage image fusion is applied to obtain a final segmented image. In Ref. [15], the author introduced a new vessel segmentation algorithm where the image is pre-processed in order to get an enhanced and smoothed image. The blood vessels are then extracted using level set. In Ref. [16], Cinsdikici et al. introduced a method that extract the blood vessels using improved ant colony method.

For study of retinal imaging, detection of blood vessels is a basic step. Although several methods are introduced for segmenting retinal blood vessel still accurate blood vessels separation is a challenging task due to vessel width disparity and low quality retinal images. Many thresholding technique have been proposed for segmenting retinal images but we have used here the local adaptive thresholding for segmenting retinal blood vessels as it can gives better segmentation performance with a lower execution time as compared to other conventional thresholding approaches. This paper presents an automated segmentation algorithm which is carried out in three stages: pre-processing, vessel extraction and post-processing. In the pre-processing stage the image is enhanced using contrast limited adaptive histogram equalization (CLAHE) [17] and then the image is thresholded using mean-C thresholding in order to detect the required blood vessels from the background. A post-processing phase is carried out in order to obtain a final segmented image. Many authors have proposed a variety of algorithm to segment the blood vessels of the retinal images but we have presents a very simple, time efficient thresholding method that gives a good accuracy as compared to many of the existing blood vessel segmentation approaches.

2. Proposed method

The proposed method for extraction of retinal blood vessels comprises of three phases: pre-processing, segmentation and post-processing. For the purpose of vessel extraction the green channel of RGB image undergo different phases. The green channel is chosen because red and blue channel suffers from poor illuminance [18]. Fig. 1 (a) and (b) shows the original RGB and green channel image respectively. All the three phases responsible for blood vessel extraction are explained below.

2.1. Pre-processing

The fundus images may suffers from nonuniform illumination, so before extraction of blood vessels pre-processing is

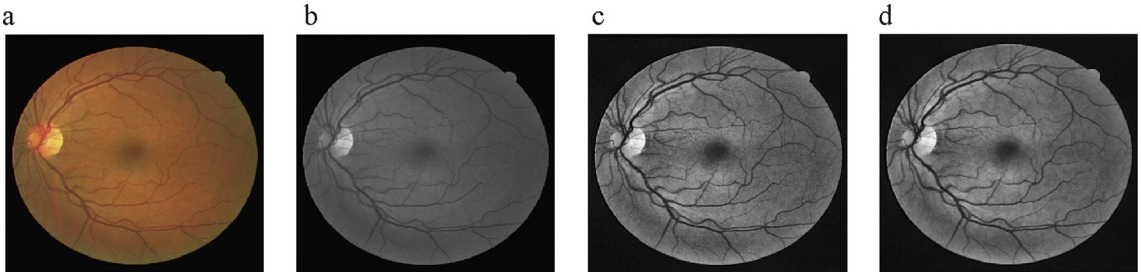

Fig. 1. (a) Original retinal image, (b) Extracted green channel image, (c) Contrast limited adaptive histogram equalized image and (d) Median filtered image.

the basic step for getting better segmentation performance. The pre-processing step includes: contrast limited adaptive histogram equalization and median filtering.

2.1.1. Contrast limited adaptive histogram equalization

Contrast limited adaptive histogram equalization (CLAHE), splits the entire space into a number of tiny sections of identical size and operates on each region **w**here the contrast of each small region is increased so that the histogram of the output image corresponds to the histogram indicated by the distribution parameter. The small neighboring regions are then combined using bilinear interpolation which suppress the artificially induced limits. Over noise amplification can be avoided by limiting the contrast of the individual homogeneous region. Fig. 1 (c) represents the CLAHE enhanced image.

2.1.2. Median filtering

The median filter is a non-linear digital filtering technique, often used to eliminate noise. This noise reduction is a distinct pretreatment footstep to upturn the properties of future treatments. The median filter is cast-off to eradicate salt and pepper noise, to smooth the image. So, it's employ in the segmentation process [19]. The median filtered image is shown in Fig. 1 (d).

2.2. Segmentation using mean-C thresholding

The black-and-white image is generated from grayscale image by setting the pixels to white whose value is beyond a certain threshold, setting the other pixels to black. Here, mean-C thresholding technique is taken where a threshold is calculated for each pixel in the image based on some local statistics such as mean, median of the neighborhood pixels and threshold is updated each time. The main advantage of this thresholding method is that it is applicable in case of badly illuminated images [20]. In mean-C thresholding (where C is a constant), for extraction of blood vessels the pixels lies in a uniform neighborhood are set to background value. The mean-C thresholding can be carried out as follows:

a. A mean filter of window size N × N is selected.
b. The enhanced image is convolved with the mean.
c. A difference image is obtain by subtracting the convolved image from enhanced image.
d. The difference image is thresholded with the constant value C.
e. The complement of the thresholded image is calculated.

Two experiments are conducted to determine the values of constant C and window size.

2.2.1. Experiment 1: To determine the value of C

In the first experiment, for selection of C, a series of values from 0.03 to 0.05 with a variation of 0.002 are taken. For every value of C, accuracy is calculated and plotted against different values of C. This is shown in Fig. 2. From the graph, it can

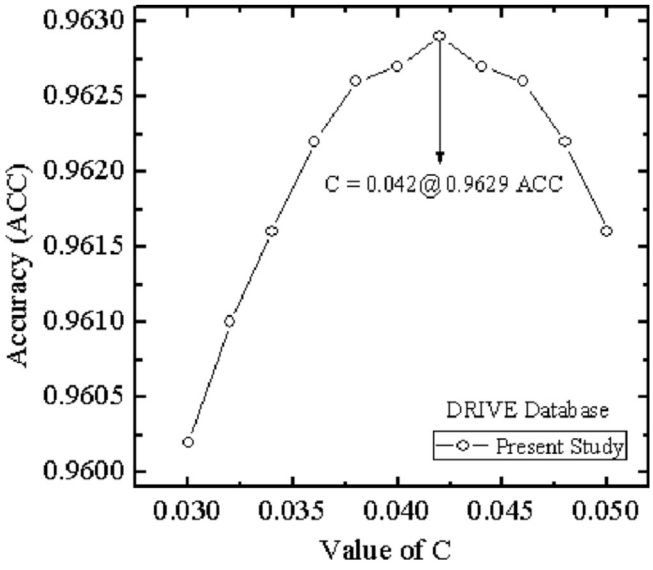

Fig. 2. Variation of accuracy with respect to constant (C).

observed that the accuracy value increases till the value of C = 0.042 and then begins to decrease. Therefore, in order to get a better result with maximum accuracy, the optimum value of C is taken as 0.042. Fig. 4 depicts the output images with different values of C. From Fig. 3 (a), it can observed that at C = 0.03 the output image includes vessels with unwanted spurious noise. At C = 0.042 the output image extract vessels with maximum accuracies 0.9629 as shown in Fig. 3 (b). For higher value of C = 0.05 less vessels are identified which is shown in Fig. 3 (c).

2.2.2. Experiment 2: To determine the value of window size

In the second experiment, by increasing the window sizes, the unnecessary black pixels are removed from the image background in a better way with filling out characters and vice versa. For selection of window size different sizes from 3 × 3 to 19 × 19 are taken and calculated the accuracies. The accuracy starts increasing from window size 3 × 3 to 13 × 13 and after 13 × 13 it starts decreasing. So, as at window size 13 × 13 maximum accuracy is obtained, the optimum window size is considered as 13 × 13. The variation of accuracy with respect to different window sizes is shown in Fig. 4.

2.3. Post-processing

The image obtained from the segmentation process contains some non-vessel which are removed with the help of a morphological cleaning operation. In this operation six neighbors containing pixels are characterized as vessel [21]. The original image and the segmentation result of DRIVE and CHASE_DB1 are shown in Fig. 5.

2.4. Algorithm for proposed method

i. Read the original RGB image.
ii. Extract the green plane of the image.

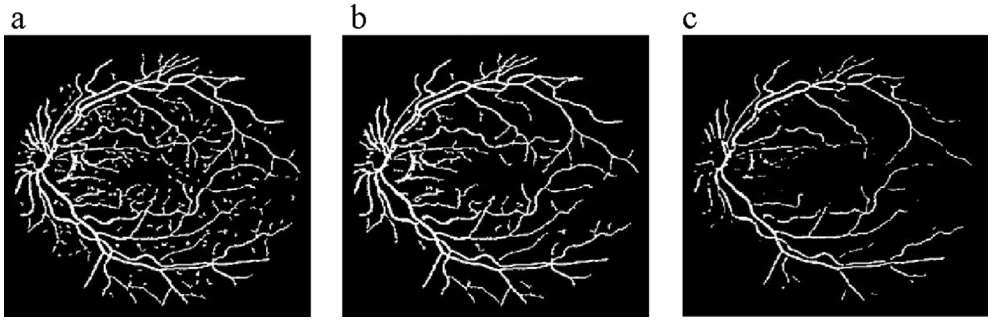

Fig. 3. Segmented image at different values of C (a) C = 0.03, (b) C = 0.042 and (c) C = 0.05.

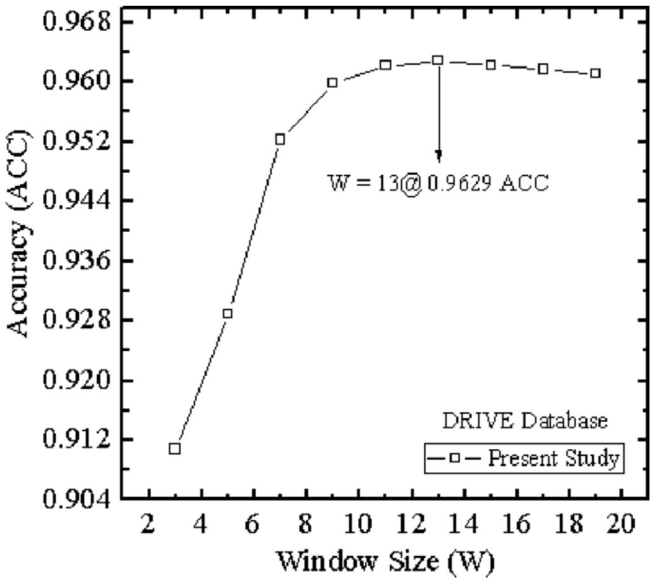

Fig. 4. Variation of accuracy with respect to window size (w).

iii. Intensify the image using CLAHE and remove noise using median filtering.
iv. Extract blood vessels using mean-C thresholding.
v. Remove the isolated pixels using morphological cleaning operation.

3. Results and discussion

By using DRIVE (Digital retinal images for vessel extraction) and CHASE_DB1 (Child heart and health study in England) the presented method's performance is appraised. The DRIVE database [22] is divided into two set: training set and test set and each data set contain twenty images. The ophthalmologists provide a single training set and two testing set of manual segmentation of the retinal images respectively. The manual segmentation suggested by the first observer of the test set is considered as ground truth. The CHASE_DB1 [23] database encompasses total of 28 images of both the left and right eyes of each child. Two sets of manual segmentation results is provided by two observers.

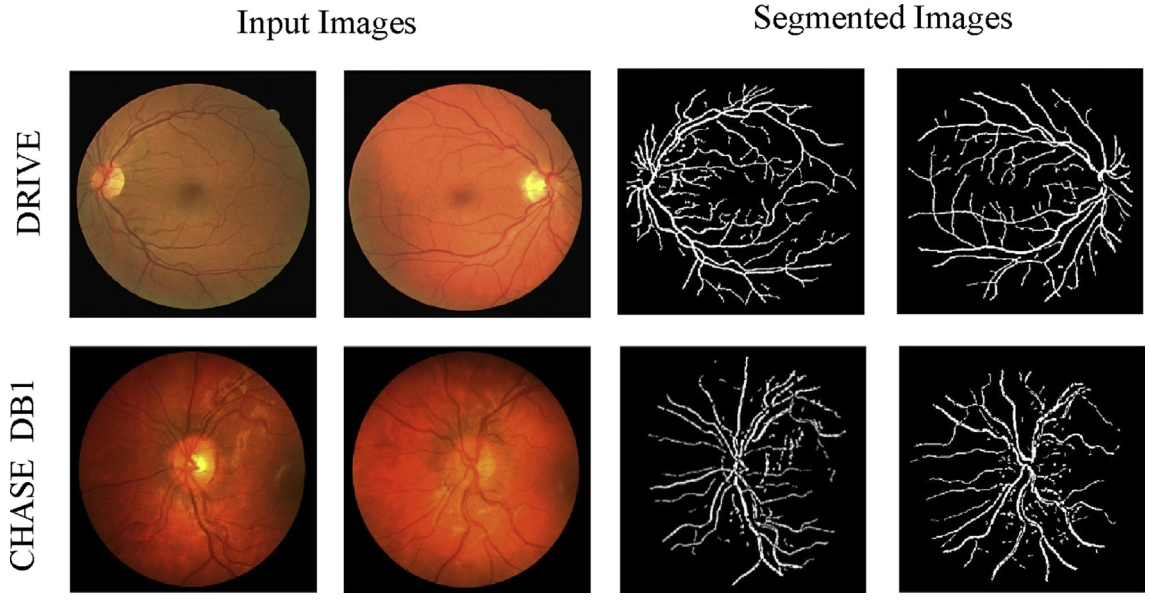

Fig. 5. Segmentation results for DRIVE and CHASE_DB1 databases.

Table 1
Mathematical parameters for performance evaluation.

Measure	Expression
TPR	$TP/TP+FN$
TNR	$TN/TN+FP$
PPV	$TP/TP+FP$
NPV	$TN/TN+FN$
FDR	$FP/FP+TN$
MCC	$TP\times TN-FP\times FN/\sqrt{(TP+FP)(TP+FN)(TN+FP)(TN+FN)}$
ACC	$TP+TN/TP+FN+TN+FP$

Table 2
Performance evaluation on the DRIVE database.

Image	TPR	TNR	PPV	NPV	FDR	MCC	ACC
1	0.776	0.979	0.789	0.978	0.160	0.762	0.962
2	0.731	0.983	0.831	0.969	0.112	0.757	0.957
3	0.700	0.972	0.736	0.964	0.183	0.676	0.944
4	0.692	0.977	0.751	0.967	0.205	0.683	0.949
5	0.694	0.984	0.799	0.963	0.167	0.686	0.951
6	0.676	0.983	0.793	0.959	0.175	0.671	0.957
7	0.695	0.969	0.687	0.966	0.245	0.694	0.952
8	0.694	0.982	0.768	0.963	0.157	0.655	0.960
9	0.729	0.982	0.759	0.967	0.210	0.667	0.954
10	0.701	0.979	0.748	0.971	0.212	0.684	0.955
11	0.709	0.965	0.660	0.969	0.273	0.642	0.940
12	0.700	0.975	0.727	0.972	0.228	0.687	0.952
13	0.695	0.977	0.758	0.963	0.198	0.676	0.956
14	0.735	0.972	0.702	0.976	0.225	0.693	0.963
15	0.740	0.960	0.688	0.979	0.211	0.631	0.944
16	0.717	0.976	0.755	0.972	0.205	0.710	0.953
17	0.680	0.983	0.792	0.970	0.148	0.712	0.967
18	0.765	0.973	0.710	0.979	0.250	0.713	0.965
19	0.820	0.978	0.771	0.983	0.183	0.776	0.965
20	0.736	0.976	0.714	0.979	0.225	0.703	0.959
Average	**0.719**	**0.976**	**0.746**	**0.970**	**0.198**	**0.694**	**0.955**

Table 3
Performance evaluation on the CHASE_DB1 database.

Image	TPR	TNR	PPV	NPV	FDR	MCC	ACC
1	0.771	0.971	0.703	0.978	0.283	0.711	0.953
2	0.698	0.981	0.768	0.967	0.231	0.674	0.952
3	0.693	0.967	0.643	0.972	0.274	0.633	0.944
4	0.684	0.982	0.793	0.966	0.206	0.684	0.952
5	0.784	0.970	0.699	0.979	0.273	0.715	0.953
6	0.701	0.981	0.769	0.974	0.230	0.706	0.958
7	0.643	0.980	0.784	0.965	0.215	0.683	0.956
8	0.694	0.976	0.756	0.958	0.243	0.649	0.948
9	0.718	0.970	0.690	0.980	0.209	0.713	0.954
10	0.659	0.973	0.732	0.958	0.267	0.644	0.963
11	0.747	0.961	0.646	0.984	0.245	0.713	0.958
12	0.681	0.986	0.761	0.959	0.238	0.702	0.951
13	0.650	0.983	0.769	0.966	0.230	0.654	0.953
14	0.741	0.981	0.726	0.972	0.273	0.759	0.957
Average	**0.704**	**0.976**	**0.731**	**0.969**	**0.244**	**0.689**	**0.954**

The performance of the proposed method is evaluated by utilizing different performance measures like true positive rate (TPR), true negative rate (TNR), positive predictive value (PPV), negative predictive value (NPV), false discovery rate (FDR), Matthews's correlation coefficient (MCC) and accuracy (ACC) [24]. Table 1 represents the vessel classification and performance matrices respectively. True positive ratio is the degree of proportion of positives that are appropriately recognized as such. True negative rate measures the ratios of negatives that are truly marked as such. Positive and negative predictive values are the quantity of positives and negatives results in the diagnosis procedure that are true positive and true negative results respectively. False discovery rate is the

Table 4
Performance comparison (DRIVE database).

Sr. No.	Methods	TPR	TNR	ACC
1	AI-Rawi et al. [3]	–	–	0.942
2	Odstrcilik et al. [5]	0.780	0.971	0.947
3	Marin et al. [6]	0.706	0.980	0.945
4	Fraz et al. [7]	0.740	0.980	0.948
5	Roychowdhury et al. [8]	0.725	0.983	0.952
6	Fraz et al. [9]	0.730	0.974	0.942
7	Azzopardi et al. [10]	0.765	0.970	0.944
8	Zhang et al. [11]	0.712	0.972	0.938
9	Roychowdhury et al. [12]	0.739	0.978	0.949
10	You et al. [13]	0.741	0.975	0.943
11	Zhao et al. [15]	0.735	0.978	0.947
12	Cinsdikici et al. [16]	–	–	0.929
13	Fraz et al. [21]	0.715	0.976	0.943
14	**Proposed method**	**0.719**	**0.976**	**0.955**

Table 5
Performance comparison (CHASE_DB1 database).

Sr. No.	Methods	TPR	TNR	ACC
1	Fraz et al. [7]	0.722	0.971	0.946
2	Roychowdhury et al. [8]	0.720	0.982	0.953
3	Azzopardi et al. [10]	0.758	0.958	0.938
4	Roychowdhury et al. [12]	0.761	0.957	0.946
5	**Proposed method**	**0.704**	**0.976**	**0.954**

Table 6
Comparative analysis of the methods in terms of time required to process image from the DRIVE database.

Method	Processing time
Marin et al. [6]	15 min
Fraz et al. [7]	2 min
Roychowdhury et al. [8]	3.115 s
Azzopardi et al. [10]	10 s
Roychowdhury et al. [12]	2.45 s
Zhao et al. [15]	2 min
Cinsdikici et al. [16]	35 s
Proposed method	**1.66 s**

Table 7
Comparative analysis of the methods in terms of time required to process image from the CHASE_DB1 database.

Method	Processing time
Roychowdhury et al. [8]	7.913 s
Roychowdhury et al. [12]	11.711 s
Proposed method	**1.98 s**

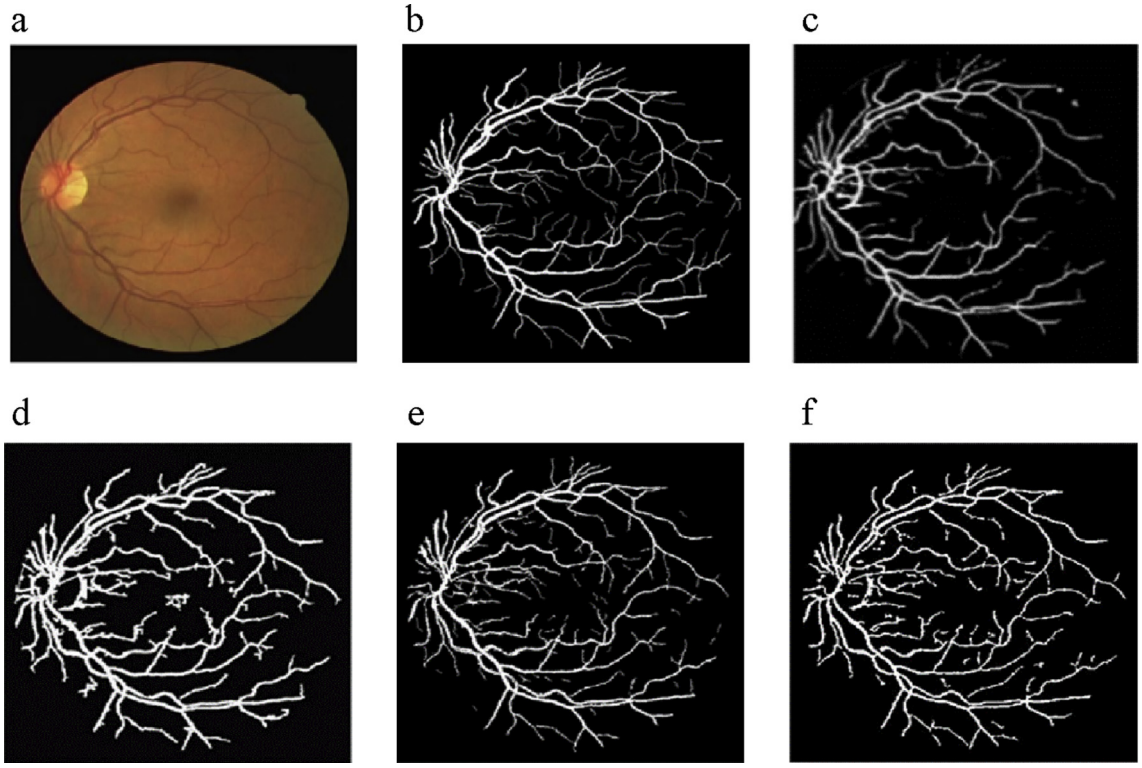

Fig. 6. Segmentation results of first retinal image from the DRIVE database using different methods (a) Original image, (b) Ground truth image of the first observer, (c) AI Rawi et al. [3], (d) Cinsdikici et al. [16], (e) Fraz et al. [9] and (f) Proposed method.

expected proportion of false positives among all significant hypotheses. The Matthews's correlation coefficient is castoff as a portion of the value of binary classifications. Accuracy is the measure of capability to classify the amount of conventionality of the resulted image to the manually segmented image.

Tables 2 and 3 shows the performance matrices for every images of DRIVE and CHASE_DB1 databases. It is perceived that the average accuracy, true positive rate and true negative rate of each of the databases is approximately equal to 0.955, 0.695 and 0.976 respectively. The high value of positive predictive value and low value of false discovery rate indicates that the vessel and nonvessel pels are marked with more exactness. Higher the value of Matthews's correlation coefficient better is the performance. The presentation of the anticipated technique is compared with the existing methodologies in respect of TPR, TNR and ACC, which are given in Tables 4 and 5 for DRIVE and CHASE_DB1 databases respectively. Tables 6 and 7 shows the comparison of proposed method with existing methods in terms of execution time for DRIVE and CHASE_DB1 databases respectively.

The performance matrices for the existing methodologies are achieved from their corresponding work. The segmentation performances of Zhang et al. [11], You et al. [13] are obtained from Zhao et al. [15] and Fraz et al. [7] and Roychowdhury et al. [12] are obtained from Azzopardi et al. [10]. The results of Al-Rawi et al. [3] is obtained from Cinsdikici et al. [16]. The outcomes of Budai et al. [14] is obtained from its original literature. The genetic algorithm matched filter optimization method [3] is not able to accurately detect the thin vessels accurately. The method introduced by Zhang et al. [11] detect some unwanted structures along with the vessels. In Ref. [13], the limitation of the method using radial projection and semi-supervised method is overestimation of thin vessels due to noise and it results in false vessel detection. In the method elaborated by Zhao et al. [15] leads to an inaccurate segmentation for some pathological images.

This paper presented a thresholding based method for vessel identification. The proposed method gives high values of different performance matrices as compared to other existing blood vessel segmentation methods. The average accuracy for the proposed method is 0.955 with TPR, TNR, PPV, NPV, FDR, and MCC of 0.719, 0.976, 0.746, 0.970, 0.198 and 0.694 respectively for DRIVE database. Similarly in CHASE_DB1 database the TPR, TNR, PPV, NPV, FDR, MCC and ACC are 0.704, 0.976, 0.731, 0.969, 0.244, 0.689, and 0.954 respectively. Fig. 6 represents the comparison of different images of proposed method with existing methods.

4. Conclusion

In this paper, we have proposed a method based on local adaptive thresholding for extraction of retinal vessels. The main contribution of the paper is the application of mean-C thresholding for retinal blood vessels extraction. The method is evaluated using two different benchmark databases. The technique attains a mean accuracies of 0.955 and 0.954 for DRIVE and CHASE_DB1 databases respectively which are better than numerous existing approaches. This automated

method can segment retinal blood vessels effectively. At the same time, the proposed method is very time efficient as it can complete the process with in an execution time of 1.66 and 1.98 s for DRIVE and CHASE_DB1 databases respectively. Together the efficacy and strength with its easiness and fast employment make the offered method a pertinent implement for being unified into a comprehensive pre-screening scheme for early identification of ophthalmological disorders.

References

[1] Harini DN, Bhaskari DL. Automatic image segmentation using grid-based Ncut and RAG. Int J Image Min 2015;1(4):279−96.
[2] El−said SA. 3D medical image segmentation technique. Int J Biomed Eng Technol 2015;17(3):232−51.
[3] Al-Rawi M, Karajeh H. Genetic algorithm matched filter optimization for automated detection of blood vessels from digital retinal images. Comput Methods Programs BIOMED 2007;87(3):248−53.
[4] Mapayi T, Viriri S, Tapamo JR. Adaptive thresholding technique for retinal vessel segmentation based on GLCM-energy information. Comput Math Methods Med 2015;2015.
[5] Odstrcilik J, Kolar R, Budai A, Hornegger J, Jan J, Gazarek J, et al. Retinal vessel segmentation by improved matched filtering: evaluation on a new high-resolution fundus image database. IET Image Process 2013;7(4):373−83.
[6] Marín D, Aquino A, Gegúndez-Arias ME, Bravo JM. A new supervised method for blood vessel segmentation in retinal images by using gray-level and moment invariants-based features. IEEE Trans Med Imaging 2011;30(1):146−58.
[7] Fraz MM, Remagnino P, Hoppe A, Uyyanonvara B, Rudnicka AR, Owen CG, et al. An ensemble classification-based approach applied to retinal blood vessel segmentation. IEEE Trans Biomed Eng 2012;59(9):2538−48.
[8] Roychowdhury S, Koozekanani DD, Parhi KK. Blood vessel segmentation of fundus images by major vessel extraction and subimage classification. IEEE J Biomed Health Inf 2015;19(3):1118−28.
[9] Fraz MM, Basit A, Barman SA. Application of morphological bit planes in retinal blood vessel extraction. J Digit Imaging 2013;26(2):274−86.
[10] Azzopardi G, Strisciuglio N, Vento M, Petkov N. Trainable COSFIRE filters for vessel delineation with application to retinal images. Med Image Anal 2015;19(1):46−57.
[11] Zhang B, Zhang L, Zhang L, Karray F. Retinal vessel extraction by matched filter with first-order derivative of Gaussian. Comput Biol Med 2010;40(4):438−45.
[12] Roychowdhury S, Koozekanani DD, Parhi KK. Iterative vessel segmentation of fundus images. IEEE Trans Biomed Eng 2015;62(7):1738−49.
[13] You X, Peng Q, Yuan Y, Cheung YM, Lei J. Segmentation of retinal blood vessels using the radial projection and semi-supervised approach. Pattern Recognit 2011;44(10):2314−24.
[14] Budai A, Bock R, Maier A, Hornegger J, Michelson G. Robust vessel segmentation in fundus images. Int J Biomed Imaging 2013;2013.
[15] Zhao YQ, Wang XH, Wang XF, Shih FY. Retinal vessels segmentation based on level set and region growing. Pattern Recognit 2014;47(7):2437−46.
[16] Cinsdikici MG, Aydın D. Detection of blood vessels in ophthalmoscope images using MF/ant (matched filter/ant colony) algorithm. Comput Methods Programs Biomed 2009;96(2):85−95.
[17] Gonzales R, Woods R. Digital image processing. Addison-Wesley Publishing Company; 1992.
[18] Walter T, Massin P, Erginay A, Ordonez R, Jeulin C, Klein JC. Automatic detection of microaneurysms in color fundus images. Med image Anal 2007;11(6):555−66.
[19] Aqeel AF, Ganesan S. Retinal image segmentation using texture, thresholding, and morphological operations. Electro/Information Technol (EIT) 2011:1−6. IEEE International Conference.
[20] Singh TR, Roy S, Singh OI, Sinam T, Singh K. A new local adaptive thresholding technique in binarization. Int J Comput Sci 2012;8(6):271−7.
[21] Fraz MM, Barman SA, Remagnino P, Hoppe A, Basit A, Uyyanonvara B, et al. An approach to localize the retinal blood vessels using bit planes and centerline detection. Comput Methods Programs Biomed 2012;108(2):600−16.
[22] Niemeijer M, Staal J, Ginneken V, Loog B, Abramoff MD. Comparative study of retinal vessel segmentation methods on a new publicly available database. Med Imaging 2004:648−56.
[23] K. U. Research. (2011, Jan.). Chase_db1 [Online]. Available: http://blogs.kingston.ac.uk/retinal/chasedb1/.
[24] Fawcett T. An introduction to ROC analysis. Pattern Recognit Lett 2006;27(8):861−74.